Dynamical Model for Chemically Driven Running Droplets

Uwe Thiele,* Karin John,† and Markus Bär‡

Max-Planck-Institut für Physik komplexer Systeme, Nöthnitzer Strasse 38, D-01187 Dresden, Germany

(Received 2 March 2004; published 9 July 2004)

We propose coupled evolution equations for the thickness of a liquid film and the density of an adsorbate layer on a partially wetting solid substrate. Therein, running droplets are studied assuming a chemical reaction underneath the droplets that induces a wettability gradient on the substrate and provides the driving force for droplet motion. Two different regimes for moving droplets—reaction-limited and saturated regime—are described. They correspond to increasing and decreasing velocities with increasing reaction rates and droplet sizes, respectively. The existence of the two regimes offers a natural explanation of prior experimental observations.

DOI: 10.1103/PhysRevLett.93.027802 PACS numbers: 68.15.+e, 47.20.Ky, 68.08.–p, 68.43.–h

It is well known that a drop of liquid can start to move if it is exposed to an external gradient. For instance, a drop of liquid immersed in another liquid that is placed in a temperature gradient will move towards the higher temperature due to Marangoni forces caused by surface tension gradients [1]. Alternatively, a temperature gradient [2] or a wettability gradient induced by a chemical grading of the substrate [3,4] causes drop motion.

Drops may also move in initially homogeneous surroundings. This is possible because such *active drops* change their surroundings and produce an internal gradient that drives their motion. One example is a drop immersed in another liquid that contains a soluble surfactant undergoing an isothermal chemical reaction at the surface of the drop [5,6]. Recent experiments found a different sort of chemically driven running droplets on solid substrates. There, the driving wettability gradient is produced by a chemical reaction at the substrate underneath the drop [7–9].

In these experiments, a small droplet of solvent is put on a partially wettable substrate. A chemical dissolved in the droplet starts to react with the substrate resulting in the deposition of a less wettable coating. The substrate below becomes less wettable than the substrate outside the droplet. Eventually, the symmetry is broken by fluctuations and the drop moves away from the "bad spot," thereby changing the substrate and leaving a less wettable trail behind (see Fig. 1). Similar phenomena can be seen in reactive (de)wetting [10], in camphor boats [11], and in the migration of reactive islands in alloying [12].

From a simple theoretical argument [13], an implicit equation for the velocity v of the droplet was derived [13]: $v = C\tan\theta^*[1 - \exp(-rL/v)]$, where r is the reaction rate, L the droplet's length, and C a constant. The dynamic contact angle θ^* is assumed to be the same at the advancing and receding ends of the droplet; i.e., the droplet profile is approximated by a spherical cap. θ^* is given by $\cos\theta^* = (\cos\theta_e^a + \cos\theta_e^r)/2$, where the static contact angles at the advancing edge θ_e^a and at the receding edge $\theta_e^r > \theta_e^a$ are different due to the chemical gradient. The expression for the velocity is found assuming a first order reaction on the substrate yielding chemical concentrations $\alpha_a = 0$ and $\alpha_r = 1 - \exp(-rL/v)$ at the respective ends of the droplet. The expression for the velocity predicts a monotone increase of the droplet velocity with the droplet length L and the reaction rate r, in line with early experimental observations [8]. Recent experiments [9] show the opposite trend; the velocity decreases with increasing drop sizes and reaction rate.

In this Letter we propose and analyze a dynamical model for self-propelled running droplets. It consists of coupled evolution equations describing the interdependent spatiotemporal dynamics of the film thickness h and a chemical concentration α that changes the substrate wettability. This model is capable of reproducing both experimentally found regimes. In particular, we identify two distinct regimes of running drops separated by a maximum of the velocity. For small droplet size or reaction rate, the chemical gradient in the drop is limited by the progress of reaction. In contrast for large droplets and fast reaction, the chemical concentration at the receding end saturates at a maximum value. Below, we show that the velocity of reaction-limited droplets increases, while the velocity of saturated droplets decreases with increasing reaction rate and drop size. In addition, we find that the dynamic contact angles at the advancing and receding edges of the droplets differ substantially. If we take into account fast diffusion of the chemical substance, the droplet velocity in the saturated regime decreases much faster, and only stationary drops are found at large

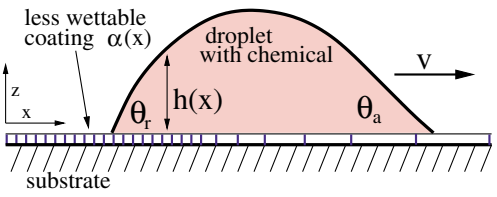

FIG. 1 (color online). Sketch of a right moving droplet driven by a chemical gradient.

 © 2004 The American Physical Society

reaction rates. The velocity of the droplets may increase [8] or decrease [9] with their volume.

A liquid layer on a smooth solid substrate is modeled by an evolution equation for the film thickness profile $h(\vec{x}, t)$ derived from the Navier-Stokes equations using long-wave approximation [14]

$$\partial_t h = -\nabla \cdot \left(\frac{h^3}{3\eta} \nabla [\gamma \Delta h + \Pi(h)] \right) \tag{1}$$

with γ and η being the surface tension and viscosity of the liquid, respectively. The disjoining pressure $\Pi(h)$ accounts for the wetting properties of the substrate [15]. We use $\Pi(h) = 2S_a d_0^2/h^3 + (S_p/l) \exp[(d_0 - h)/l]$ [16,17], where S_a and S_p are the apolar and polar components of the total spreading coefficient $S = S_a + S_p$, respectively, $d_0 = 0.158$ nm is the Born repulsion length, and l is a correlation length [16]. We choose $S_a > 0$ and $S_p < 0$, thereby combining a stabilizing long-range van der Waals and a destabilizing short-range polar interaction. The latter contains the influence of the coating and crucially influences the static contact angle [16]. Such a model allows for solutions representing static droplets with a finite mesoscopic equilibrium contact angle sitting on an ultrathin precursor film.

To account for the varying wettability caused by the chemical reaction, we let the polar part of the spreading coefficient S_p depend linearly on the coating density, i.e., on the concentration $\alpha(\vec{x}, t)$ of a chemical species adsorbed at the substrate,

$$S_p = S_p^0 \left(1 + \frac{\alpha}{g'} \right) < 0. \tag{2}$$

The equilibrium contact angle θ_e is given by $\cos\theta_e = S/\gamma + 1$ [16]. This implies that θ_e increases with α; i.e., the coated substrate is less wettable. The constant S_p^0/g' defines the magnitude of the wettability gradient. Note that Eq. (2) corresponds to the linear relation between $\cos\theta_e$ and α assumed in [8,9,13].

The evolution of the chemical concentration on the substrate is modeled by a reaction-diffusion equation for $\alpha(\vec{x}, t)$,

$$\partial_t \alpha = R(h, \alpha) + d' \Delta \alpha, \tag{3}$$

where the function $R(h, \alpha)$ describes the reaction that changes the wettability of the substrate and the second term allows for diffusion along the substrate. The main results, however, are obtained without diffusion. As a reaction term we choose

$$R(h, \alpha) = r' \Theta(h - h_0) \left(1 - \frac{\alpha}{\alpha_{\max}} \right). \tag{4}$$

The time scale of the reaction is defined by the rate constant r'. It is assumed that the reaction occurs only underneath the droplet; this is modeled by the step function $\Theta(h - h_0)$. The value of h_0 is chosen slightly larger than the thickness of the precursor film. The chemical concentration of the coating saturates at a value $\alpha_{\max}$, because the reaction is assumed to be fast enough to produce a complete adsorption layer. Changes in details of R like the replacement of the step function by an explicit proportionality to h do not affect our results qualitatively. The physical motivation behind the actual choice is a fast equilibration of the reactant concentration within the moving droplet, caused by diffusion and convective motion within the droplet.

We rewrite Eqs. (1)–(4) by introducing scales $3\gamma\eta/l\kappa^2$, $\sqrt{l\gamma/\kappa}$, $\alpha_{\max}$, and l for t, $\vec{x}$, α, and h, respectively. Then, $\kappa = (|S_p|/l) \exp(d_0/l)$ is the dimensionless spreading coefficient. Defining the dimensionless reaction rate $r = 3r'\gamma\eta/l\kappa^2$, diffusion constant $d = 3d'\eta/\kappa l^2$, wettability gradient $g = g'/\alpha_{\max}$, and ratio of the effective molecular interactions $b = 2S_a d_0^2/l^3\kappa$, we obtain from Eqs. (1)–(4) the dimensionless coupled evolution equations for the thickness profile h and the substrate coverage α

$$\partial_t h = -\nabla \cdot \left\{ h^3 \nabla \left[\Delta h + \frac{b}{h^3} - \left(1 + \frac{\alpha}{g} \right) e^{-h} \right] \right\}, \tag{5}$$

$$\partial_t \alpha = r\Theta(h - h_0)(1 - \alpha) + d\Delta\alpha. \tag{6}$$

In the one-dimensional version of Eqs. (5) and (6), we calculate by use of continuation techniques [18] two-dimensional running droplets moving with constant speed [19]. Figure 2 shows the constant profiles of such moving droplets [2(a) and 2(b)] together with the corresponding concentration profiles for α [2(c) and 2(d)] for two qualitatively different regimes (prominently visible in the α profiles). In Figs. 2(a) and 2(b) the streamlines indicate the convective motion in the droplets.

In Figs. 2(a) and 2(c) the limiting factor for the motion is the small reaction rate. The reaction time is long compared to the viscous time scale; i.e., the droplet passes too fast for the coverage α to approach its saturation

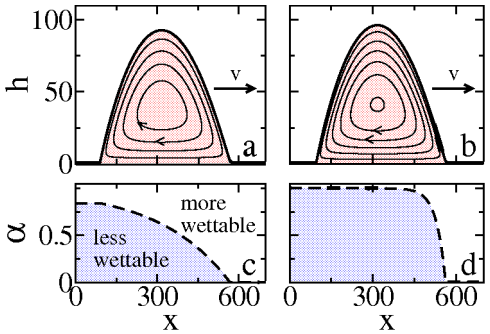

FIG. 2 (color online). Profiles of the droplet $h(x, t)$ [(a), (b)] and the concentration α of the coating [(c),(d)] in the two qualitatively different running droplet regimes. (a),(c) Reaction-limited regime at $r = 0.0001$ moving with velocity $v = 0.026$. (b),(d) Saturated regime at $r = 0.001$ with $v = 0.032$. The streamlines plotted in (a) and (b) indicate the convective motion inside the droplet in the comoving frame [19]. The remaining parameters are $g = 1.0$, $d = 0.0$, $b = 0.5$, and the droplet volume is 30 000.

value. In the case $d = 0$, we can estimate the value of α at the receding end to be $\alpha_r = 1 - \exp(-rL/v)$ where L is the length of the droplet. We call this regime reaction limited. In Figs. 2(b) and 2(d) the reaction at the receding edge has reached its saturating value, i.e., $\alpha_r \approx 1$ and $rL/v \gg 1$. After the droplet has passed, the concentration α stays at the saturation level. We call this regime saturated. One cannot exactly predict where the transition between the regimes occurs, because the velocity of the droplet and the driving wettability gradient determine each other dynamically. We found that in both regimes the advancing contact angle is substantially smaller than the receding one. This contradicts the assumption of identical dynamic contact angles in the approximate theory [13].

We have tested that the above model also allows for stationary moving droplets in three dimensions (Fig. 3) by integrating Eqs. (5) and (6) in time starting from adequate initial conditions [20]. After a transient the droplets approach constant shape and velocity. We show resulting droplets for the reaction-limited [Figs. 3(a) and 3(c)] and the saturated [Figs. 3(b) and 3(d)] regimes. Both drops have an oval shape with an asymmetry between the advancing and the receding parts that is stronger in the saturated regime due to the larger wettability gradient.

A closer analysis of the one-dimensional version of Eqs. (5) and (6) gives insight into the properties of the running droplets and their existence and stability conditions. Figure 4(a) shows the droplet velocity in dependence of the reaction rate r without and with diffusion. The dependence of the velocity on the reaction rate r for the running droplets is nonmonotonic. There exists a value r_m where the velocity is maximal. The case $r < r_m$ [$r > r_m$] defines the reaction-limited [saturated] regime.

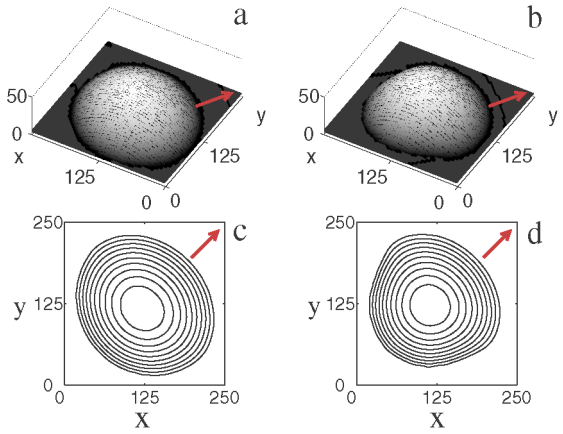

FIG. 3 (color online). Moving drops in three dimensions. Shown are the film thickness profiles in the (a) reaction-limited and (b) saturated regimes. (c),(d) The corresponding contour lines. The velocity converged to $v \approx 0.018$ and $v \approx 0.044$, respectively. The direction of movement is indicated by arrows, the parameters correspond to Figs. 2(a) and 2(c), respectively, and the droplet volume is 7.5×10^5. Only a part of the computational domain size of 500×500 is shown.

The velocity increase for $r < r_m$ is easily explained by the increasing value of α_r at the back of the drop caused by the faster reaction. The decreasing velocity for $r > r_m$ originates from a slow increase of α in the contact region at the front of the drop, while α at the back remains constant at its saturation value ($\alpha_r \approx 1$). We have also studied the case where the diffusion of α is sizable. There, the rapidly produced α diffuses to the substrate in front of the droplet and diminishes the driving gradient between the front and the back of the drop. The velocity curve is similar for small r but decreases even faster beyond the maximum and drops to zero at large enough r; there, no running droplets are found anymore. The latter phenomenon is reminiscent of observations of moving spots in reaction-diffusion systems of an activator-inhibitor type [21–23]. Therein, a transition from moving to stationary droplets (drift pitchfork bifurcation) occurs when the inhibitor is produced too fast.

Figures 4(b) and 4(c) give, respectively, the tangents of the measured advancing and receding dynamic contact angles ($\tan\theta_{a/r}$) and their differences $\Delta\tan\theta_{a/r} = \tan\theta_{a/r} - \tan\theta_e(\alpha_{a/r})$ from the static contact angles as a function of the droplet's velocity in the case $d = 0$. All contact angles given correspond to the mesoscopic contact angles measured at the inflection points of the drop profiles. To determine the static contact angle we take the value of α at the inflection point to calculate a space independent polar spreading coefficient in Eq. (5).

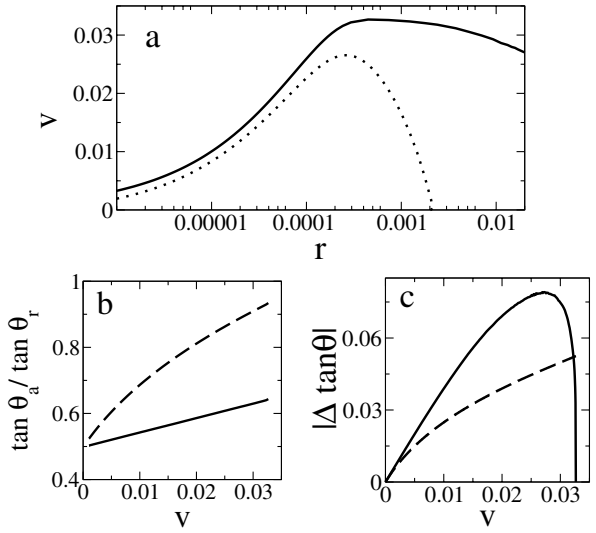

FIG. 4. Characterization of running droplets stationary in a comoving frame. Shown are (a) the velocity v dependent on the reaction rate r (logarithmic scale) without ($d = 0$, solid line) and with ($d = 1.0$, dotted line) diffusion; (b) the tangents of the advancing θ_a (solid line) and receding θ_r (dashed line) dynamic contact angles in the reaction-limited regime; (c) the absolute value of the difference of $\tan\theta_a$ (solid line) and $\tan\theta_r$ (dashed line) and the tangents of the static contact angle $\theta_e(\alpha)$ at the corresponding α values. Also in (c) only the reaction-limited regime $r < r_m$ is shown where always $\theta_a > \theta_e(\alpha_a)$ and $\theta_r < \theta_e(\alpha_r)$. The remaining parameters are as in Fig. 2.

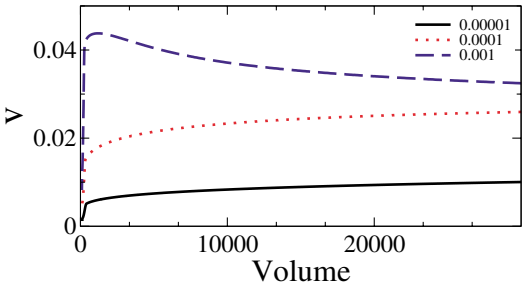

FIG. 5 (color online). The transition between (i) the reaction-limited and (ii) the saturated regimes is most clearly seen in the dependence of velocity v on drop size, i.e., droplet volume V. Curves are plotted for different reaction rates r (see legend). The remaining parameters are as in Fig. 2.

Figure 4(b) shows that the two dynamic contact angles may differ quite strongly. However, a comparison of Figs. 4(b) and 4(c) shows that the difference between the static and the dynamic contact angles is much smaller.

Experimentally, an important measure is the dependence of droplet velocity on droplet length or volume [8,9] shown here in Fig. 5. For small reaction rates r we find that the velocity increases with drop length. The increase becomes more pronounced for larger r. This corresponds to the reaction-limited regime *and* the experiments in [8]. Upon a further increase of r, the curve shows a velocity maximum at an intermediate drop size. For bigger drops, the velocity decreases monotonically, similar to the observations of [9]. Inspection of the corresponding profiles suggests that one is again in the saturated regime.

To conclude, we have modeled chemically driven moving droplets by a dynamical model consisting of coupled evolution equations for the film thickness profile and the concentration of a surface coating that is produced underneath the droplet. This model exhibits moving droplets with constant speed and shape in two and three dimensions. A systematic analysis of the velocities of two-dimensional droplets allows us to distinguish the reaction-limited and saturated regimes, which are characterized by a respective increase and decrease of droplet velocities with increasing droplet size or reaction rate. The behavior in the saturated regime indicates that the velocity of the droplets in our model depends not only on the values of the chemical coating at the advancing and receding ends of the droplet, but is in addition determined by the concentration profiles of α near the contact lines. The two regimes offer a natural explanation of the conflicting experimental observations in [8,9].

Financial support by German-Israeli Foundation (GIF) is gratefully acknowledged.

*Electronic addresses: thiele@mpipks-dresden.mpg.de; http://www .uwethiele.de
†Electronic address: john@mpipks-dresden.mpg.de
‡Electronic address: baer@mpipks-dresden.mpg.de

[1] M. G. Velarde, Philos. Trans. R. Soc. London A **356**, 829 (1998).
[2] F. Brochard, Langmuir **5**, 432 (1989).
[3] E. Raphaël, C.R. Acad Sci. Ser. II **306**, 751 (1988).
[4] M. K. Chaudhury and G. M. Whitesides, Science **256**, 1539 (1992).
[5] A. Y. Rednikov, Y. S. Ryazantsev, and M. G. Velarde, Phys. Fluids **6**, 451 (1994), and references therein.
[6] A. S. Mikhailov and D. Meinköhn, in *Lecture Notes in Physics*, edited by L. Schimansky-Geier and T. Pöschel (Springer, Berlin, 1997), Vol. 484, p. 334.
[7] C. D. Bain, G. D. Burnetthall, and R. R. Montgomerie, Nature (London) **372**, 414 (1994).
[8] F. Domingues Dos Santos and T. Ondarcuhu, Phys. Rev. Lett. **75**, 2972 (1995).
[9] S.W. Lee, D.Y. Kwok, and P. E. Laibinis, Phys. Rev. E **65**, 051602 (2002).
[10] D.W. Zheng, W. Wen, and K. N. Tu, Phys. Rev. E **57**, R3719 (1998).
[11] Y. Hayashima *et al.*, Phys. Chem. Chem. Phys. **4**, 1386 (2002).
[12] A. K. Schmid, N. C. Bartelt, and R. Q. Hwang, Science **290**, 1561 (2000).
[13] F. Brochard-Wyart and P.-G. de Gennes, C.R. Acad. Sci. Ser. IIB **321**, 285 (1995).
[14] A. Oron, S. H. Davis, and S. G. Bankoff, Rev. Mod. Phys. **69**, 931 (1997).
[15] J. N. Israelachvili, *Intermolecular and Surface Forces* (Academic Press, London, 1992).
[16] A. Sharma, Langmuir **9**, 861 (1993).
[17] U. Thiele *et al.*, Colloid Surf. A **206**, 135 (2002).
[18] E. J. Doedel *et al.*, *AUTO97: Continuation and Bifurcation Software for Ordinary Differential Equations* (Concordia University, Montreal, 1997).
[19] The stationary profiles are computed in a box of length S and in a comoving frame $x - vt$. Boundary conditions are $h(S) = h(0)$, $d\partial_x\alpha(z = S) + v\alpha(z = S) = 0$, and $\partial_x\alpha(z = 0) = 0$ stemming from $\alpha(S) \to 0$ as $S \to \infty$ and the assumption of constant α profile behind the drop towards $-\infty$. The streamlines in Fig. 2 correspond to lines of constant stream function $\psi(x, z)$ in the comoving frame given by
$$\psi(x, z) = \left(\frac{3z^2h}{2} - \frac{z^3}{2}\right)\partial_x p(h, \alpha) + vz, \qquad (7)$$
where the pressure $p(h, \alpha)$ corresponds to the expression in square brackets in Eq. (5).
[20] The integration in time starts from a liquid "cylinder" with a small added noise using periodic boundary conditions. Initially, the α field is slightly shifted to fix the direction of movement. In the course of the simulation it is set to its initial value far behind the droplet. An explicit scheme is used on 96×96 and 128×128 grids and for drops moving in different directions with respect to the underlying grid.
[21] K. Krischer and A. Mikhailov, Phys. Rev. Lett. **73**, 3165 (1994).
[22] M. Or-Guil *et al.*, Phys. Rev. E **57**, 6432 (1998).
[23] H. U. Bödeker *et al.*, Phys. Rev. E **67**, 056220 (2003).